Available online at www.sciencedirect.com

SCIENCE DIRECT®

Polymer 47 (2006) 1661–1666

polymer

www.elsevier.com/locate/polymer

Effect of nano-$CaCO_3$ on polymorphic behavior in syndiotactic polystyrene for non-isothermal crystallization

Ming Lu, Weihua Zhou, Kancheng Mai *

Materials Science Institute, Key Laboratory of Polymeric Composites and Functional Materials, The Ministry of Education, School of Chemistry and Chemical Engineering, Sun Yat-sen University, Guangzhou, Guangdong 510275, People's Republic of China

Received 9 September 2005; received in revised form 21 December 2005; accepted 16 January 2006

Abstract

Syndiotactic polystyrene (*s*PS)/nano-$CaCO_3$ composites were prepared on a twin screw extruder for the first time. Differential scanning calorimeter and wide-angle X-ray diffraction were used to investigate the effect of maximum melting temperature (T_{max}) and the content of nano-$CaCO_3$ on the crystal forms and melting behavior of *s*PS for non-isothermal crystallization. The results indicated that the increasing T_{max} decreases the crystallization temperature of *s*PS and facilitates the formation of β-crystal. The addition of nano-$CaCO_3$ changes the melting behavior and crystal form of melt-crystallized *s*PS and facilitates the formation of β-crystal. The increase in the content of nano-$CaCO_3$ decreases crystallization temperature of *s*PS and increases the content of β-crystal, which was similar to the effect of increasing T_{max}. Pure β-crystal in *s*PS/nano-$CaCO_3$ composites can be obtained at lower melting temperature due to the effect of nano-$CaCO_3$.

Keywords: Syndiotactic polystyrene; Nano-$CaCO_3$; Polymorphic behavior

1. Introduction

Syndiotactic polystyrene (*s*PS) was widely studied since successful synthesis in 1985 [1] because of its high melting point, fast crystallization rate, good chemical and thermal resistance, etc. It is well known that *s*PS exhibits complex polymorphism and multiple melting behavior. Generally, four crystal forms, termed α-, β-, γ- and δ-crystal have been described. Melt-crystallization at most accessible temperatures produces solidified *s*PS containing both α- and β-crystal forms of various fractions determined by experiment conditions. De Rosa et al. [2–4] suggested that the crystallization of the α- and β-crystal forms is mainly dependent on the maximum melting temperature (T_{max}) of the melt. At high T_{max}, the *s*PS always crystallizes in the β-crystal form. At lower T_{max}, the formed crystalline modification depended on the crystalline form of the starting material of *s*PS. They proposed that the T_{max} effect on the formation of polymorphism was attributed to the memory effect of α-crystal. Woo and his co-workers [5] suggested that the formation of polymorphism in *s*PS was primarily determined by crystallization kinetics. At lower nucleation barrier, the crystallization of *s*PS tends to form α-crystal. When the residual nuclei are absent at high enough T_{max}, *s*PS crystallized as β-crystal from due to high nucleation barrier. Coexistence of α- and β-crystals generally results in multiple melting behaviors. Woo and his co-workers [6–11] did much work on the multiple melting behaviors of *s*PS. When resolution of DSC is high enough, four melting endothermic peaks, labeled as P-I, P-II, P-III and P-IV in the increase of temperature of melting peaks in the order, were observed in melt-crystallized *s*PS. The peaks of P-II and P-IV are attributed to the melting of α-crystal while the peaks of P-I and P-III are corresponding the melting of β-crystal [7]. Woo [5] and Wang [12] studied the equilibrium melting temperature (T_m^o) of α- and β-crystals using linear and non-linear Hoffman–Weeks plots, respectively, and found that the T_m^o of β-crystal is higher than that of α-crystal.

The studies on polymorphism of *s*PS in its blends and composites have been reported. It was observed that *s*PS blending with miscible polymer, such as PPO and aPS, favors the formation of β-crystal [3,13–15]. For *s*PS filled with clay, the study results of both Chang [16] and Wang [17] indicated that clay makes *s*PS decline to yield β-crystal. However, Wu et al. [18–20] found that addition of clay favors the formation of α-crystal in *s*PS.

As one of the most important mineral fillers, nano-calcium carbonate (nano-$CaCO_3$) is commonly used to improve the

---

* Corresponding author. Tel./fax: +86 20 84115109.
E-mail address: cesmkc@zsu.edu.cn (K. Mai).

0032-3861/$ - see front matter © 2006 Elsevier Ltd. All rights reserved.
doi:10.1016/j.polymer.2006.01.039

mechanical properties (strength and toughness) of PP [21–25], PVC [26,27] and HDPE [28,29]. Many studies indicated that nano-$CaCO_3$ can induced the formation of β-crystal of PP [30,31]. However, *s*PS composites filled with nano-$CaCO_3$ has not been reported. In this article, *s*PS/nano-$CaCO_3$ composites were prepared on a twin screw extruder for the first time. The main aim of this paper is to make clear of the effect of nano-$CaCO_3$ on the polymorphism and melting behavior of *s*PS matrix during non-isothermal crystallization.

2. Experiment

2.1. Materials

Syndiotactic polystyrene (*s*PS) is friendly provided by Dow Chemical Co. with M_w of 226,000 and M_w/M_n of 2.8, determined by GPC. Nano-$CaCO_3$ treated with stearic acid is kindly supplied by Guang Ping Nano Technology Group Ltd, Guangdong, China. The average particle size range, determined by TEM, is of 40–60 nm.

2.2. Preparation of sPS/nano-$CaCO_3$ composites

*s*PS pellet was pre-mixed with 2.5 and 5 wt% nano-$CaCO_3$ after being dried. Then the pre-mixed compounds were melted and extruded in a twin-screw SJSH-Z-30 extruder (Nanjing Rubber and Plastics Machinery Co. Ltd, China) at the temperature of 280 °C with a screw speed of 100 rpm. The extruded products were frozen in-line in a water bath and cut into pellet form by a pelletizer. The composites containing 2.5 and 5 wt% nano-$CaCO_3$ were named as *s*PS-CC2.5 and *s*PS-CC5, respectively. The pure *s*PS was extruded under the same condition as the *s*PS/nano-$CaCO_3$ composites.

2.3. Characterizations

2.3.1. Differential scanning calorimeter

Non-isothermal crystallization and melting behavior of *s*PS and *s*PS/nano-$CaCO_3$ composites were investigated on a Perkin–Elmer 7 differential scanning calorimeter (DSC). Temperature calibration was performed using an indium standard ($T_m^o = 156.6$ °C and $\Delta H_f^o = 28.5$ J/g). The sample was heated to the maximum melting temperature (T_{max}) at a heating rate of 100 °C/min and melted for 10 min to eliminate the thermal history and then cooled it to room temperature at a cooling rate of 10 °C/min. After that, the sample was subjected to reheating at a rate of 10 °C/min to 290 °C. Both the DSC crystallization and the melting curves were recorded for further analysis. All measurements were carried out in nitrogen atmosphere. Each sample was about 5 mg.

2.3.2. Wide-angle X-ray diffraction

The samples of neat *s*PS and *s*PS/nano-$CaCO_3$ composites for wide-angle X-ray diffraction (WAXD) were prepared in DSC cell with the same thermal history as DSC non-isothermal crystallization experiment. The samples were determined by using a Rigaku D/max 2200vpc diffractometer (Cu Kα radiation, $\lambda = 1.542$ Å). The step scanning rate was 2°/min. The X-ray source was operated at a voltage of 40 kV and a filament current of 30 mA.

3. Results and discussion

3.1. Effect of nano-$CaCO_3$ on the polymorphic behavior of sPS

The DSC crystallization thermograms of neat *s*PS and *s*PS/nano-$CaCO_3$ composites crystallized non-isothermally after melting at temperature of 280 °C (A) and 320 °C (B) are shown in Fig. 1. It is observed that the effect of nano-$CaCO_3$ on crystallization behavior of *s*PS is dependent on the maximum melting temperature (T_{max}). The crystallization temperature of *s*PS in its composites is lower than that of *s*PS at $T_{max} = 280$ °C. However, the addition of nano-$CaCO_3$ has no influence in the crystallization temperature of *s*PS at $T_{max} = 320$ °C. Therefore, the decrease in the crystallization temperatures of *s*PS is higher than that of composites as T_{max} increased from 280 to 320 °C. These results indicated that the

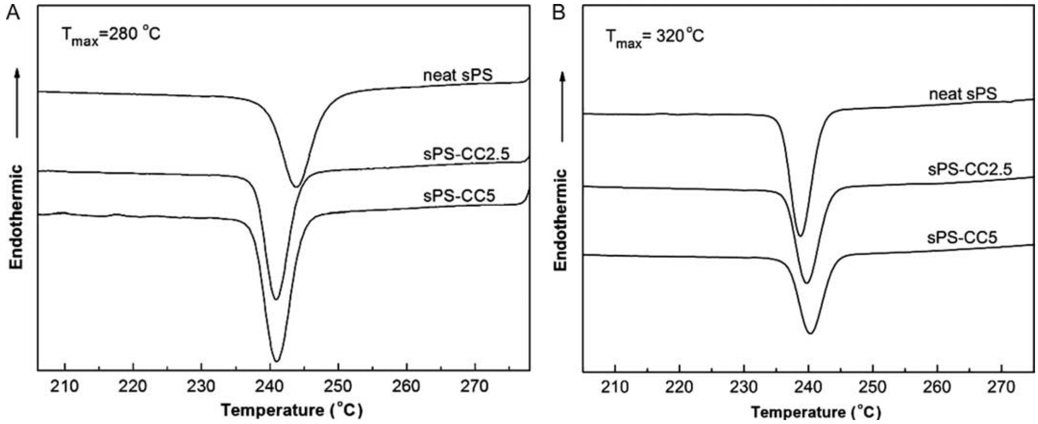

Fig. 1. DSC crystallization thermograms of neat *s*PS and *s*PS/nano-$CaCO_3$ composites crystallized non-isothermally after melting at temperatures of 280 °C (A) and 320 °C (B) for 10 min.

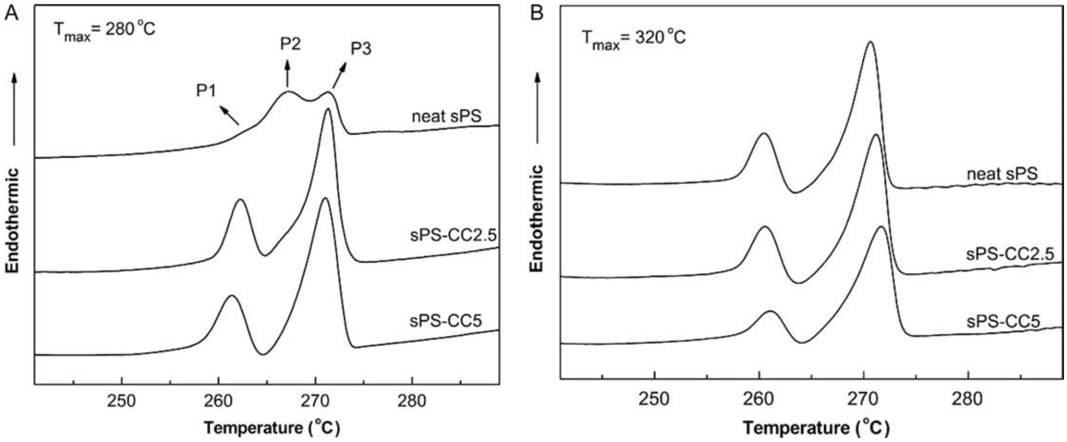

Fig. 2. DSC melting thermograms of neat *s*PS and *s*PS/nano-$CaCO_3$ composites crystallized non-isothermally after melting at temperature of 280 °C (A) and 320 °C (B) for 10 min.

effect of adding nano-$CaCO_3$ on the crystallization behavior of *s*PS is the same as the effect of increasing T_{max}, decreasing the crystallization temperatures of *s*PS.

The DSC melting thermograms of neat *s*PS and *s*PS/nano-$CaCO_3$ composites at $T_{max}=280$ °C (A) and 320 °C (B) are shown in Fig. 2. It is interesting that the effect of nano-$CaCO_3$ on *s*PS melting behaviors is also dependent on T_{max}. At $T_{max}=280$ °C, significant difference between the melting behaviors of *s*PS and its composites is observed. For the neat *s*PS, two melting peaks and a small shoulder peak on the lower temperature side were observed in the melting curve, labeled as P1, P2, and P3 (from low to high temperature in the order), respectively. The addition of 2.5 wt% nano-$CaCO_3$ dramatically increases the intensity of P1 and P3 and decreases the intensity of P2. The P2 was weakened from a strong separate peak into a very tiny shoulder peak between P1 and P3. When the content of nano-$CaCO_3$ increases to 5 wt%, the P2 completely vanished, and both P1 and P3 remain. However, only two peaks, P1 and P3, appear in DSC melting curves of both neat *s*PS and composites at $T_{max}=320$ °C. That is, the addition of nano-$CaCO_3$ has little effect on the melting behavior of *s*PS at higher T_{max}. Compared Fig. 2A with B, it is suggested that the addition of nano-$CaCO_3$ or the increase in T_{max} produce the same effect on the melting behavior of *s*PS.

The corresponding WAXD patterns were shown in Fig. 3. From Fig. 3A, stronger diffraction peaks of α-crystal ($2\theta\approx6.8$, 11.7, 14.1, 15.6 and 18.0°) [2,32] and weaker characteristic peaks of β-crystal ($2\theta\approx6.2$, 10.4, 12.4, 13.7, 18.6, and 21.3°) [2,33,34] were observed for neat *s*PS at $T_{max}=280$ °C, indicating that melt-crystallization from $T_{max}=280$ °C produces solidified *s*PS containing higher content of α-crystal and a small quantity of β-crystal. However, the addition of 2.5 wt% nano-$CaCO_3$ substantially diminished the intensities of α-crystal diffraction peaks. As the content of nano-$CaCO_3$ was increased to 5 wt%, the characteristic peaks of α-crystal entirely vanished and only the typical peaks of β-crystal was observed. The results indicated that the content of α-crystal in melt-crystallized *s*PS dramatically decreased with increasing content

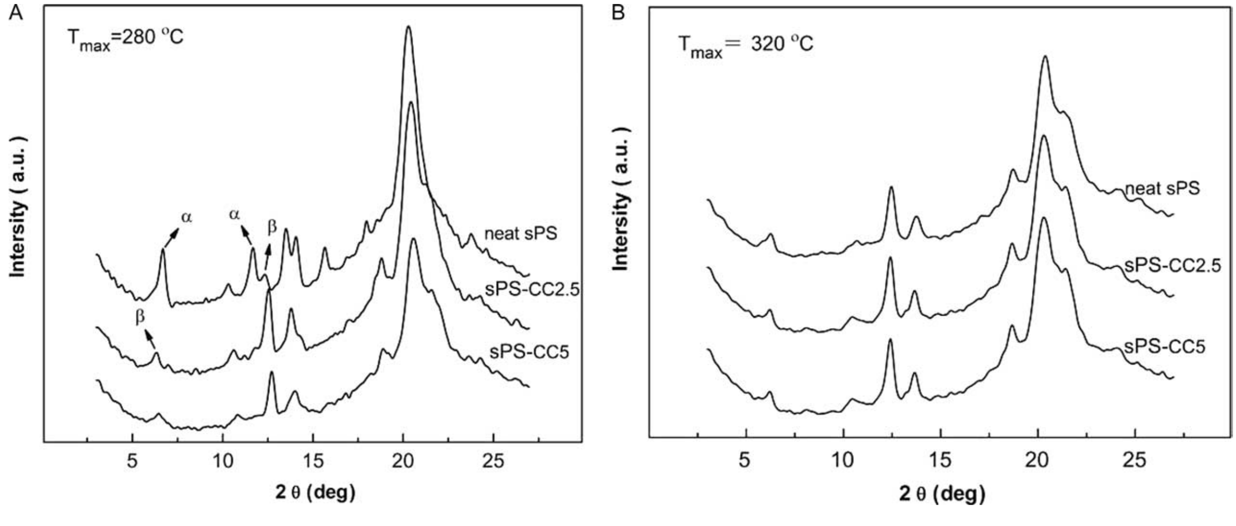

Fig. 3. WAXD patterns of neat *s*PS and *s*PS/nano-$CaCO_3$ composites crystallized non-isothermally after melting at temperature of 280 °C (A) and 320 °C (B) for 10 min.

of nano-$CaCO_3$. It is suggested that the addition of nano-$CaCO_3$ favored the formation of β-crystal of *s*PS at lower T_{max}. This effect was strengthened with increasing nano-$CaCO_3$ content. However, only characteristic peaks of β-crystal were observed in the WAXD patterns of both neat *s*PS and its composites at higher T_{max} (shown in Fig. 3B). It is illustrated that pure β-crystal can be produced for both neat *s*PS and *s*PS/nano-$CaCO_3$ composites. Therefore, the addition of nano-$CaCO_3$ has no influence on the crystal form of *s*PS at $T_{max}=320$ °C. Because the addition of nano-$CaCO_3$ favors the formation of β-crystal of *s*PS, the T_{max} at which the pure β-crystal is produced in its composites is lower than that of neat *s*PS.

Based on the results of DSC and WAXD, P1 in DSC melting curves was considered as a result of the melting of β-crystal, while P2 was associated with melting of α-crystal. P3 was attributed to a result of melting of β-crystal in *s*PS crystallized after melting high T_{max} or a result of melting of α- and β-crystal in *s*PS crystallized after melting low T_{max}. It is suggested that the decrease in the crystallization temperatures of *s*PS by adding nano-$CaCO_3$ and the differences of melting behavior between *s*PS and its composites are attributed to higher fractions of β-crystal in the composites.

3.2. Dependence of melting temperature on the polymorphic behavior of sPS

The WAXD patterns of neat *s*PS crystallized non-isothermally after melting at different T_{max} are shown in Fig. 4A. From the WAXD data, the percentage of the α-crystal content (Pα%) was evaluated with the following approximate relation [2]:

$$P\alpha(\%) = \{[1.8A(11.7)/A(12.4)]/[1 + 1.8A(11.7)/A(12.4)]\} \times 100\%$$

The relationship of T_{max} and the content percentage of α-crystal in the crystalline of neat *s*PS was displayed in Fig. 4B. It can be observed that α-crystal is the domain crystal form while β-crystal only occupied a small portion in melt-crystallized *s*PS at lower T_{max}. As the T_{max} increases from 290 to 296 °C, the fraction of α-crystal almost significantly decrease. At T_{max} above 296 °C, no α-crystal was observed and β-crystal became the exclusive crystal form in melted crystallized *s*PS.

Fig. 4C showed the changes of crystallization onset temperature (T_c^{on}), crystallization peak temperature (T_c^p) and crystallization enthalpy (ΔH_c) of neat *s*PS with increasing T_{max}. It can be observed that the T_c^{on} and T_c^p decreased while the ΔH_c increased with increasing T_{max}. It is interesting to observe dramatic changes at T_{max} between 293 and 296 °C. When the T_{max} is below 293 °C or above 296 °C, the T_c^{on} and T_c^p, and ΔH_c change slightly with increasing T_{max}. However, as the T_{max} increased from 293 to 296 °C, the T_c^{on} and T_c^p significantly decreased and the ΔH_c remarkably increased. These phenomena may be explained as follows: at lower T_{max}, there remained a small quantity of crystal in melt, which acted as nucleation

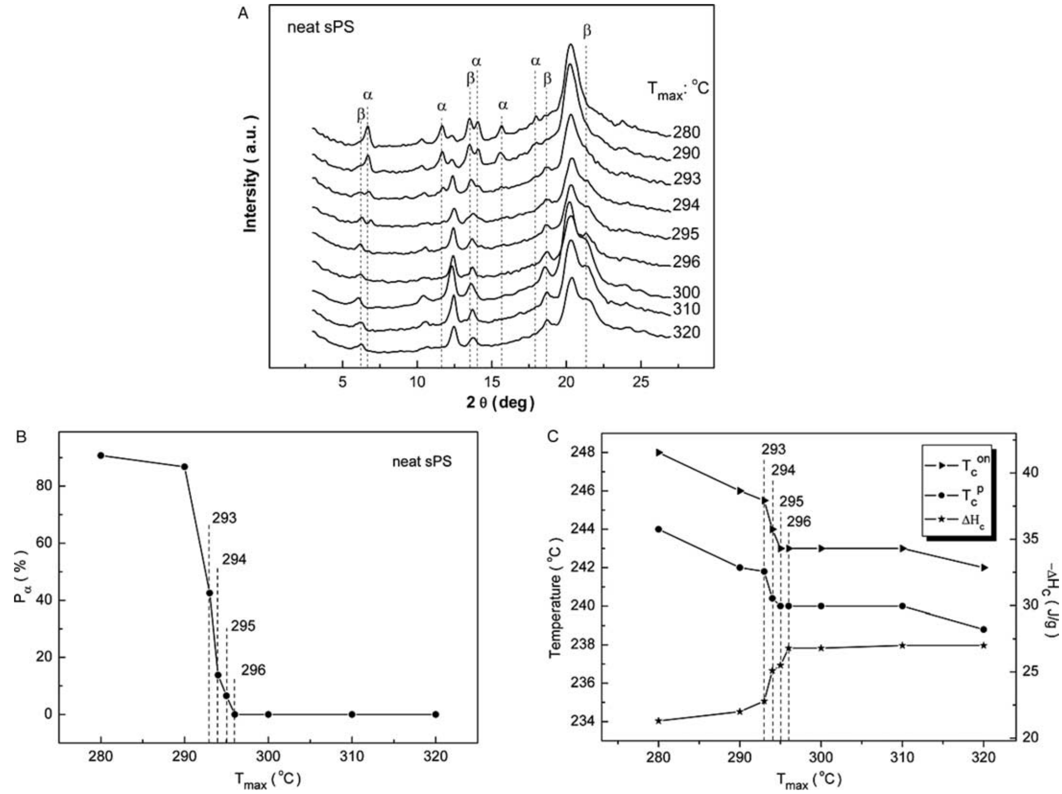

Fig. 4. (A) WAXD patterns of neat *s*PS crystallized non-isothermally after melting at different T_{max} for 10 min. (B) Relationship of Pα% and T_{max} for neat *s*PS. (C) Relationship of T_c^{on}, T_c^p, ΔH_c and T_{max} for neat *s*PS.

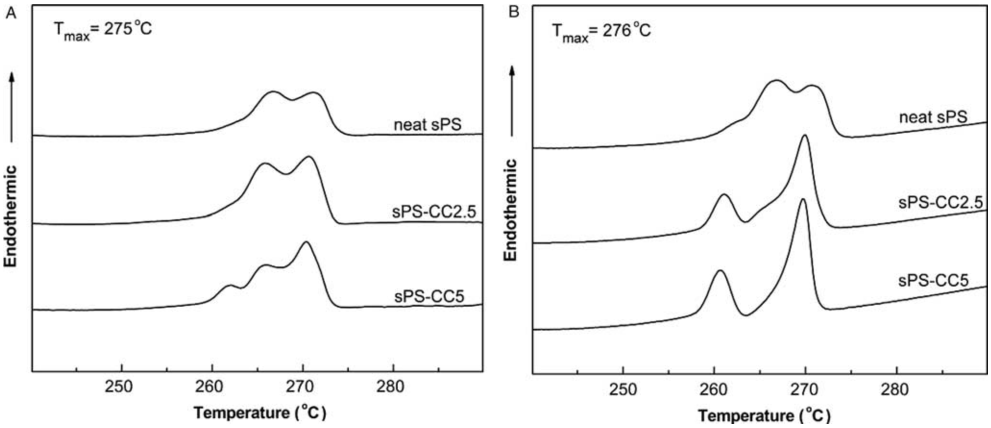

Fig. 5. DSC melting thermograms of neat *s*PS and *s*PS/nano-$CaCO_3$ composites crystallized non-isothermally after melting at temperatures of 275 °C (A) and 276 °C (B) for 10 min.

seeds during the crystallization. So the self-nucleation of the residual nuclei led to higher T_c^{on} and T_c^p. Unmelted residual nuclei has no contribution to the ΔH_c. With increasing T_{max}, the residual nuclei in melt reduced gradually which resulted in the decrease of T_c^{on} and T_c^p. When the residual nuclei were completely annihilated at higher T_{max}, the T_{max} had no influence on the T_c^{on} and T_c^p. Completely melted residual nuclei crystallized during cooling process and lead to increase in the ΔH_c. Therefore, the ΔH_c remarkably increased as the T_{max} increased from 293 to 296 °C. Since, the T_m^o of α-crystal is lower than that of β-crystal [5,12], the melting nuclei might be of α-crystal. As α-crystal was completely melted above 296 °C, the memory of α-crystal entirely vanished. As a result, the β-crystal became the exclusive crystal form in melt-crystallized *s*PS.

Above results indicated that the increasing T_{max} decreases the crystallization temperature and the content of α-crystal of *s*PS while increased the ΔH_c. A considerable changes were observed at T_{max} between 290 and 296 °C. It is suggested that, co-existence of α- and β-crystal at various fraction in melt-crystallized *s*PS at lower T_{max} is attributed to the presence of originally unmelted α-crystal left in the melt, acting as nucleation seeds of α-crystal crystallization. At higher T_{max}, the formation of pure β-crystal in melt-crystallized *s*PS is attributed to the absence of nucleation seeds of α-crystal crystallization due to the completely be melted of α-crystal in the melt. The significant decreasing crystallization temperature and increasing ΔH_c of *s*PS are dependent on the formation of more β-crystal in melt-crystallized *s*PS. Our results indicated that the crystallization temperature of *s*PS decreases with increasing T_{max} and favors the formation of β-crystal in melt-crystallized *s*PS. The addition of nano-$CaCO_3$ also decreases the crystallization temperature of *s*PS and facilitates β-crystal. Therefore, it is suggested that the crystal form of melt-crystallized *s*PS is dependent of the crystallization temperature of *s*PS. The decrease in the crystallization temperature facilitates the formation of β-crystal.

3.3. Dependence of melting temperature on the polymorphic behavior of nano-$CaCO_3$/sPS composites

Fig. 5 shows the DSC melting thermograms of neat *s*PS and *s*PS/nano-$CaCO_3$ composites at $T_{max}=275$ °C (A) and 276 °C (B). It can be seen from Fig. 5A that the two main melting peaks (P2 and P3) and a very weak shoulder peak (P1) at lower temperature region of P2 were observed in both neat *s*PS and its composite containing 2.5 wt% nano-$CaCO_3$ (*s*PS-CC2.5). For the composite containing 5 wt% nano-$CaCO_3$ (*s*PS-CC5), the intensity of P1 significantly increased. When the T_{max} was increased to 276 °C, the melting behavior of neat *s*PS is the same as that of *s*PS at $T_{max}=275$ °C. However, the melting behaviors of composites are dramatically different from that of composites at $T_{max}=275$ °C and *s*PS at $T_{max}=276$ °C. In the composites, P2 was greatly weakened to an extremely small shoulder peak between P1 and P3, especially composite containing 5 wt% nano-$CaCO_3$. However, the intensities of P1 and P3 distinctly increase. The P1 is attributed to α-crystal and P2 is corresponded to β-crystal. It is suggested that most of the α-crystal vanished and a large mount of β-crystals were formed in *s*PS/nano-$CaCO_3$ composites when T_{max} increases from 275 to 276 °C.

The changes of T_c^{on}, T_c^p and ΔH_c of melt-crystallized *s*PS-CC2.5 composites with T_{max} were displayed in Fig. 6. It is observed that when the T_{max} increases from 275 to 276 °C, the ΔH_c greatly increased while the T_c^{on} and T_c^p dramatically decreased. However, the T_{max} has little influence on the ΔH_c and crystallization temperatures of *s*PS when T_{max} is above 276 °C. This phenomenon was similar to that of neat *s*PS crystallized melting at T_{max} from 293 to 294 °C. It is suggested that the crystallization behavior and crystal forms of *s*PS are influenced by the addition of nano-$CaCO_3$. The addition of nano-$CaCO_3$ favors the formation of β-crystal of *s*PS. The T_{max} at which most of residual α nuclei melted in its composites was about 18 °C lower than that in *s*PS. When the T_{max} increased from 275 to 276 °C, most of the residual α-crystal was melted. Therefore, β-crystal can be obtained in *s*PS/nano-$CaCO_3$ composites at T_{max} much lower than that of *s*PS.

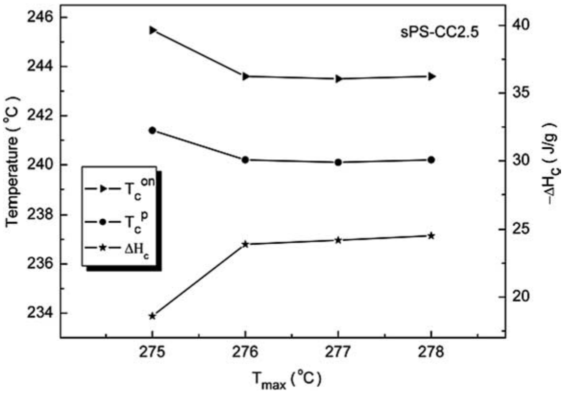

Fig. 6. Relationship of T_c^{on}, T_c^p, ΔH_c and T_{max} for *s*PS-CC2.5.

4. Conclusion

The investigation of the melting behavior and crystal forms of *s*PS and *s*PS/nano-$CaCO_3$ composites crystallized non-isothermally after melting at different maximum melting temperature (T_{max}) indicated that the increase in T_{max} decreases the crystallization temperature of *s*PS and facilitates the formation of β-crystal. When the T_{max} is below 293 °C or above 296 °C, the T_{max} has little influence on crystallization temperature and enthalpy of *s*PS. As the T_{max} increased from 293 to 296 °C, the crystallization temperature of *s*PS significantly decreased while the crystallization enthalpy remarkably increased. The addition of nano-$CaCO_3$ produces great changes in the melting behavior and crystal forms of melt-crystallized *s*PS, decreasing the crystallization temperature of *s*PS and favoring the formation of β-crystal, which was similar to the effect of increasing T_{max}. Because of the effect of nano-$CaCO_3$, pure β-crystal in *s*PS/nano-$CaCO_3$ composites can be obtained at lower T_{max}.

References

[1] Ishihara N, Semiya T, Kuramoto M, Uoi M. Macromolecules 1986;19:2464.
[2] Guerra G, Vitagliano VM, De Rosa C, Petraccone V, Corradini P. Macromolecules 1990;23:1539.
[3] Guerra G, De Rosa C, Vitagliano VM, Petraccone V, Corradini P. J Polym Sci, Part B: Polym Phys 1991;29:265.
[4] De Rosa C, De Ballesteros OR, Di Gennaro M, Auriemma F. Polymer 2003;44:1861.
[5] Ho RM, Lin CP, Tsai HY, Woo EM. Macromolecules 2000;33:6517.
[6] Woo EM, Wu FS. Macromol Chem Phys 1998;199:2041.
[7] Sun YS, Woo EM. Macromolecules 1999;32:7836.
[8] Woo EM, Sun YS, Lee ML. Polymer 1999;40:4425.
[9] Woo EM, Sun YS, Yang CP. Prog Polym Sci 2001;26:945.
[10] Lin RH, Woo EM. Polymer 2001;41:121.
[11] Sun YS, Woo EM. Polymer 2001;42:2241.
[12] Wang C, Hsu YC, Lo CF. Polymer 2001;42:8447.
[13] Guerra G, De Rosa C, Vitagliano VM, Petraccone V, Corradini P, Karasz FE. Polym Commun 1991;32:30.
[14] Woo EM, Wu FS. J Polym Sci, Part B: Polym Phys 1998;36:2725.
[15] Chiu FC, Peng CG. Polymer 2002;43:4879.
[16] Wu HD, Tseng CR, Chang FC. Macromolecules 2001;34:2992.
[17] Wang ZM, Chung TC, Gilman JW, Manias E. J Polym Sci, Part B: Polym Phys 2003;41:3173.
[18] Wu TM, Hsu SF, Wu JY. J Polym Sci, Part B: Polym Phys 2002;40:736.
[19] Wu TM, Hsu SF, Wu JY. J Polym Sci, Part B: Polym Phys 2003;41:560.
[20] Wu TM, Hsu SF, Chien CF, Wu JY. Polym Eng Sci 2004;44:2288.
[21] Thio YS, Argon AS, Cohen RE, Weinberg M. Polymer 2002;43:3661.
[22] Chan CM, Wu J, Li JX, Cheung YK. Polymer 2002;43:2981.
[23] Zuiderduin WCJ, Westzaan C, Hue'tink J, Gaymans RJ. Polymer 2003;44:261.
[24] Zhang Q, Yu Z, Xie X, Mai Y. Polymer 2004;45:5985.
[25] Dangtungee R, Yun J, Supaphol P. Polym Test 2005;24:2.
[26] Xie X, Liu Q, Li R, Zhou X, Zhang Q, Yu Z, et al. Polymer 2004;45:6665.
[27] Zhang L, Chen X, Li C. J Mater Sci 2005;40:2097.
[28] Bartczak Z, Argon AS, Cohen RE, Weiberg M. Polymer 1999;40:2347.
[29] Lazzeri A, Zebarjad SM, Pracella M, Cavalier K, Rosa R. Polymer 2005;46:827.
[30] Lin Z, Zhang Y, Huang Z, Mai K, Zeng H. J Appl Polym Sci 2004;91:2443.
[31] Huang Z, Lin Z, Mai K. Plast Rubber Compos 2004;33:343.
[32] Chatani Y, Shimane Y, Ijitsu T, Yukinari T. Polymer 1993;34:1625.
[33] De Rosa C, Rapacciuolo M, Guerra G, Petraccone V, Corradini P. Polymer 1992;33:1423.
[34] De Rosa C. Macromolecules 1996;29:8460.